# Assessing response times of an alluvial aquifer experiencing seasonally variable meteorological inputs


Lamine Boumaiza[1,2], Romain Chesnaux[1,2], Julien Walter[1,2], Fethi Meghnefi[1]

[1] Département des Sciences Appliquées, Université du Québec à Chicoutimi, Saguenay, Québec, G7H 2B1, Canada

[2] Centre d'études sur les ressources minérales, Groupe de recherche Risque Ressource Eau, Université du Québec à Chicoutimi, Saguenay, Québec, G7H 2B1, Canada

Corresponding author: lamine.boumaiza@uqac.ca (L. Boumaiza)

**ABSTRACT**

This study aims to assess the spatiotemporal distribution of the response times of an alluvial aquifer experiencing seasonally variable meteorological inputs and to investigate the aquifer characteristics that influence its response times. The sliding cross-correlogram approach was used in this study to correlate the amount of water infiltrating the subsurface with changes in water table levels that were monitored at six piezometers. The results showed a significant variation of aquifer response times over the study area; this finding indicates that the hydraulic behavior of an aquifer may differ from one location to another within the same aquifer. Aquifer response times were found to be influenced by the variations of the vadose zone thickness. These variations, however, were not observed to be a significant factor controlling the spatiotemporal changes in the aquifer response times. Instead, it was the intensity of the vertical inflow events and the local recharge rate that were found to exert an impact on the spatiotemporal variation of the aquifer response times. It was assumed that large amounts of vertical inflow increase the soil's volumetric water content above the water table, leading to higher values of hydraulic conductivity of unsaturated soils, thus contributing to shortening aquifer response times. A better understanding of the effects of aquifer characteristics on aquifer response times is useful for groundwater resource management.

**Keywords:** Cross-correlation; Sliding-window; Water table level; Water infiltration; Snowmelt; Canada

## 1 Introduction

Granular deposits are increasingly exploited worldwide for many activities, either through sand extraction for manufacturing cement construction of facilities, or, given their potential to provide important quantities and quality of groundwater, as water supply reservoirs. It has long been recognized that understanding the functioning of these granular aquifers is highly relevant—especially in developing regions—for the long-term management and protection of water resources. Detailed knowledge of granular deposits is made difficult because of: (i) the heterogeneity of aquifer sediments, which often present a complex spatial distribution of granular sizes with varying hydrogeological properties (Boumaiza et al., 2015; Hsien-tsung et al., 2010; Vienken and Dietrich, 2011), and (ii) the heterogeneity of landscape catchment characteristics, including vegetation cover and topography (Brodersen et al., 2000; Lozano-Parra et al., 2015; Uchida et al., 2006). Liquid precipitation infiltrating into the subsurface influences the soil water content, altering water flow. Infiltration manifests as changes in (i) aquifer water table level, (ii) spring discharge, and/or (iii) neighboring river levels (Bailly-Comte et al., 2008; Bouchaou et al., 2002; Chiaudani et al., 2017; Duvert et al., 2015; Rathay et al., 2018). A delayed response has been commonly observed between a change in water table level and its corresponding input precipitation event. Indeed, the time lag between a precipitation event and the water table response to this event (this time lag is what constitutes the aquifer response time) has been reported in many studies across a wide range of aquifers, either in fractured-rock systems (Cai and Ofterdinger, 2016; Padilla and Pulido-Bosch, 1995; Panagopoulos and Lambrakis, 2006; Pavlić and Parlov, 2019; Tam et al., 2004) or in alluvial granular deposits (Chiaudani et al., 2017; Duvert et al., 2015; Imagawa et al., 2013). The relationship, between the occurrence of a precipitation event and the water table fluctuations that are subsequently manifested, provides information on the hydrogeological characteristics of vadose zone, the water transit-time through the vadose zone, and the aquifer's groundwater recharge processes (Allocca et al., 2015; Carretero and Kruse, 2012; Jeong and Park, 2017; Owor et al., 2009; Turkeltaub et al., 2015). An aquifer's response time is known to be shorter during the high water table level period (wet season), and longer during the low water table level period (dry season) (Larocque et al., 1998; Lee et al., 2006). Imagawa et al., (2013) investigated the response time of the alluvial aquifer of Takashima, Japan, according to three contrasting climate patterns. They established that the aquifer response time in dry conditions was at least twice as long as the response time during wet periods of abundant rainfall. Lee et al. (2006) demonstrated the existence of a direct, positive, and proportional relationship between the vadose zone thickness and the aquifer response time, i.e., when the thickness increases, the response time increases. The effect of the vadose zone thickness is further enhanced by its degree of saturation; when the thickness increases, the degree of saturation diminishes. In turn, a reduced saturation of the vadose zone diminishes the overall hydraulic conductivity of the vadose zone and increases the aquifer response time. Delbart et al. (2014) showed that the aquifer response time is more closely related to the saturation of the aquifer vadose zone, and this saturation has been observed to be linked to greater rainfall intensity, explaining the consequent shorter response time of their examined aquifer. It can be understood that an aquifer's behavior in terms of its response time is controlled by the climate and by subsurface conditions; thus, the variation over time of these conditions leads to the variation over time of an aquifer's response time.

Most of the studies on aquifer response times have been conducted on sites where the inflow originates mainly from rainfall (Allocca et al., 2015; Cai and Ofterdinger, 2016; Carretero and Kruse, 2012; Chiaudani et al., 2017; Delbart et al., 2014; Duvert et al., 2015;

Lee et al., 2006; Owor et al., 2009; Panagopoulos and Lambrakis, 2006; Pavlić and Parlov, 2019; Tam et al., 2004; Turkeltaub et al., 2015). The spatiotemporal dynamic of aquifer response times, and the effect of aquifer characteristics on these response times, have more rarely been investigated in northern regions characterized by diverse meteorological inputs occurring over long periods of time. The main objectives of the present study are: (i) to characterize the spatiotemporal distribution of the response times of an aquifer subject to diverse meteorological inputs, and (ii) to investigate the aquifer characteristics that influence its response times. The Saint-Honoré aquifer, located in the Saguenay-Lac-Saint-Jean (SLSJ) region of Quebec (Canada), was selected to conduct the present study. This aquifer is subject to a typical northern humid climate, characterized by diverse seasonal meteorological episodes (i.e., snowfall, snowpack, snowmelt, and rainfall). The Saint-Honoré aquifer has been the object of numerous hydrogeological research studies (Boumaiza, 2008; Boumaiza et al., 2020b, 2020a, 2019, 2017, 2015; Chesnaux and Stumpp, 2018; Labrecque et al., 2020; Tremblay, 2005). However, no study had yet been conducted with the specific objectives of the present study. Knowledge of aquifer response times makes it possible to determine groundwater recharge times; thus, assessing the variation over time of aquifer response times may further contribute to improving groundwater resource management. In the present study, this aquifer is considered as a box that controls the relationship between the two studied time-series of data, i.e., (1) the amount of water available for infiltration into the subsurface and (2) the water table level. Here, water infiltrating into the subsurface displaces the existing pore water by pushing it deeper down until it eventually penetrates into the saturated zone (Duffy and Gelhar, 1986; Horton and Hawkins, 1965).

# 2 Materials and Methods

## 2.1 Study area

### 2.1.1 *Geographic location and climate*

The aquifer of Saint-Honoré belongs to the SLSJ region of Quebec, Canada (Figure 1). The Saint-Honoré aquifer covers a surface of approximately 60 $km^2$; this extended surface posed some difficulty in studying the entire aquifer system. However, a portion of this aquifer located around the Saint-Honoré Airport (Figure 1) presents an appropriately distributed number of piezometers that have been monitored for a number of months. This section of the aquifer is considered in the present study as being representative of the Saint-Honoré aquifer. It is covered by forest, agricultural lands and urban areas, including the small regional Saint-Honoré Airport (Figure 1). Precipitations over the study area are captured as rainfall and snowfall. The study area experiences heavy snow accumulation with limited water infiltration during the winter-spring seasons (from November to March/April). The snowfall accumulated as snowpack during this cold period is subject to occasional melting in response to occasional increases in temperature, before melting completely during the snowmelt period—generally occurring in April/May—when 4-5 months of accumulated snowpack is rapidly transformed into water available for infiltration. The snowmelt episode is subsequently followed by rainy events over the summer-autumn seasons. The Saint-Honoré aquifer captures a uniformly distributed mean annual precipitation of 930 mm (standard deviation of 21 mm), including an equivalent of 320 mm of water representing the mean annual snow accumulation. In the present study, the term “vertical inflow” is used to designate the amount of rainfall or snowmelt generated from snowpack, as well as the sum of rainfall and snowmelt amounts when they occur simultaneously.

### 2.1.2 *Geology*

The study area was marked by the last glaciation event which began approximately 85,000 years ago—during the early stage of the Wisconsinan period—and ended approximately 7,000 years ago (Parent and Occhietti, 1988). During its retreat toward the north, the last glacier covering the SLSJ region left behind a discontinuous and heterogeneous layer of till, terminal moraines and glaciolacustrine/fluvioglacial deposits which were derived from basement rocks deposits (Daigneault et al., 2011; Lasalle and Tremblay, 1978; Pagé, 1999). Following the glacier's retreat, the SLSJ region was invaded by the Laflamme Sea (~11,800 years ago; Lasalle and Tremblay, 1978). This marine invasion led to the deposition of semi-continuous material mainly composed of clayey silt and silty clay. Overlying these fine-grained sediments are the post-glacial granular sediments (i.e., littoral/deltaic deposits) that were deposited during the regression of the Laflamme Sea. The Saint-Honoré aquifer was deposited at the mouth of the Valin River that flowed north to south into the post-glacial Laflamme Sea. The Quaternary material thus deposited then formed an unconfined aquifer having a depth of approximately 50 m; it is mainly composed of sand with silt overlying a Precambrian Crystalline bedrock belonging to the Canadian Precambrian Shield (Hébert and Lacoste, 1998; Lasalle and Tremblay, 1978; Laurin and Sharma, 1975).

### 2.1.3 *Hydrogeological background*

Recharge in the Saint-Honoré aquifer is mainly dominated by snowmelt that usually occurs in the late-spring season. A mean recharge rate of 70% was estimated for this aquifer using a method based on stable isotopes (Boumaiza et al., 2020b; Chesnaux and Stumpp, 2018). This rate is representative of the summer-autumn period, as during the winter-spring period, there is negligible snowmelt and the surface soil is usually frozen and covered by thick snowpack (up to 1 m), which acts as a barrier to water infiltration. With an average effective porosity of 42% calculated from in-situ/laboratory soil sample analyses (Boumaiza, 2008; Boumaiza et al., 2015), the unconfined aquifer of Saint-Honoré constitutes an important groundwater reservoir, and is subject to intense use, supplying 34% of the total groundwater for domestic and commercial use in the SLSJ region (CERM-PACES, 2013). The granular deposits of the Saint-Honoré aquifer are composed of highly permeable material; indeed, the average hydraulic conductivity obtained from soil sample granulometry and by in situ variable head permeability tests was evaluated to be $2.44\times10^{-2}$ cm/s (Boumaiza et al., 2015; Labrecque et al., 2020). The bedrock specifically located under the Saint-Honoré aquifer has not been very well documented, but based on research conducted in neighboring regions (CERM-PACES, 2013; Chesnaux and Elliott, 2011), it may be hydraulically connected with the overlying granular deposits through the possible presence of fractures in the top layer of the bedrock. The topography of the water table of the St Honoré aquifer replicates and generally runs parallel to the surface topography, before discharging primarily into the Saguenay River (Boumaiza et al., 2021; Meinken and Stober, 1997; Tremblay, 2005; Walter et al., 2017).

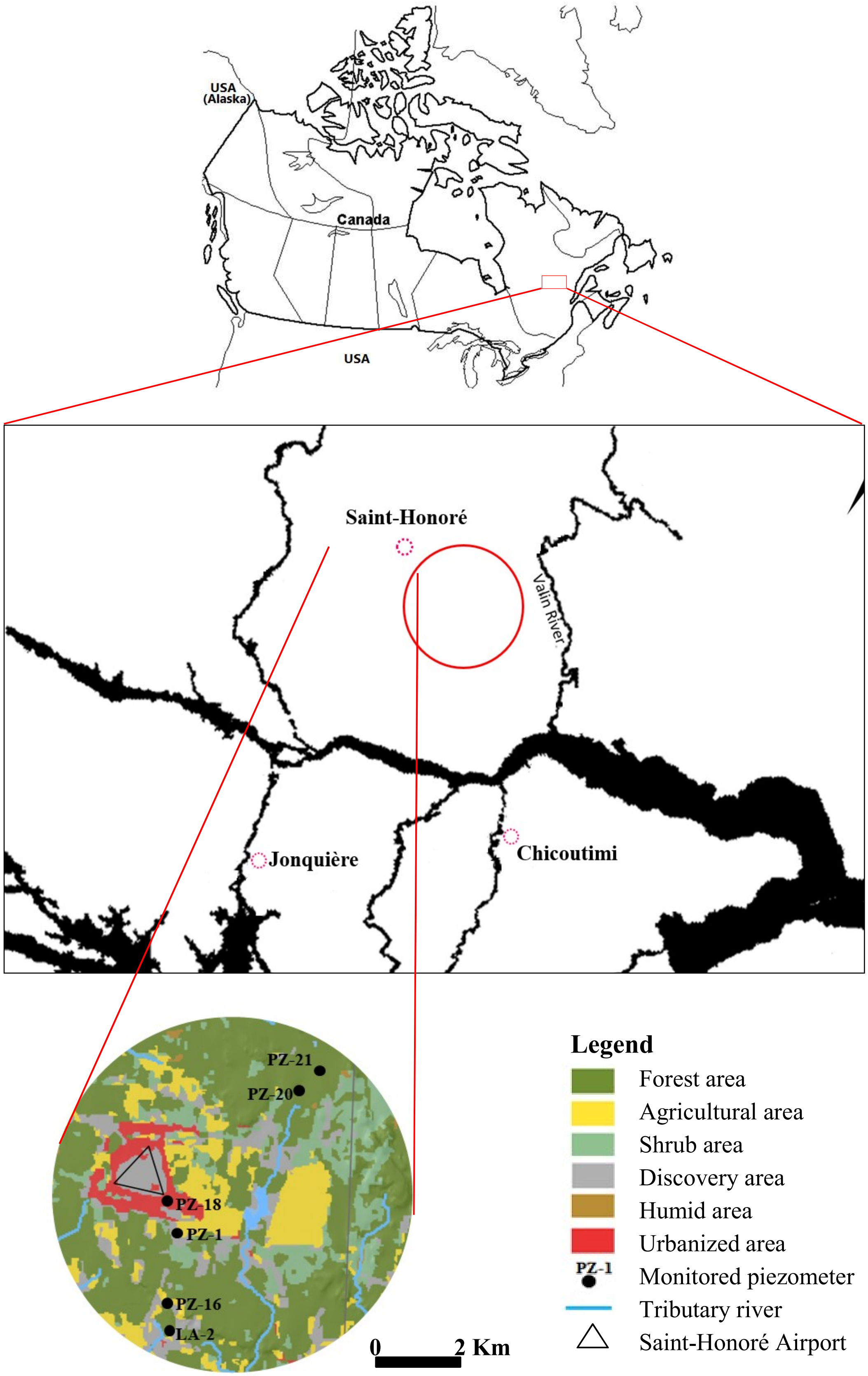


Figure 1. Geographic location of the study area and the monitored piezometers.

## 2.2 **Data acquisition**

### 2.2.1 ***Water table level***

For this study, the water table levels were monitored at six piezometers (LA-2, PZ-1, PZ-16, PZ-18, PZ-20 and PZ-21) over a period ranging from 2 November 2016 to 8 December 2017, except for PZ-1 whose monitoring started one week later, on 9 November 2016. The locations of the six monitored piezometers are shown in Figure 1. These piezometers were implemented by the company *Laboratoires S.L. inc*. in 1981 as part of a hydrogeology study; the specific characteristics at each piezometer's location (sediment stratigraphy, ground surface elevation, elevation of the piezometer bottom, elevation of the screened section and mean water table elevation) are presented in Figure 2. For this study, the six piezometers were equipped with pressure sensors to monitor local fluctuations of the water table at 15-minute time intervals. These fluctuations are considered to be representative of natural conditions because they are not affected by anthropogenic activities such as excessive pumping in the wells and/or leaking pipelines sometimes observed in urbanized areas. Because agricultural activities in the study area are limited to the summer season and are based on natural irrigation, lesser impacts are expected of agricultural activities on water table fluctuations. Data collected were converted to mean daily values in order to be consistent with precipitation data that are also recorded on a daily basis (see next section).

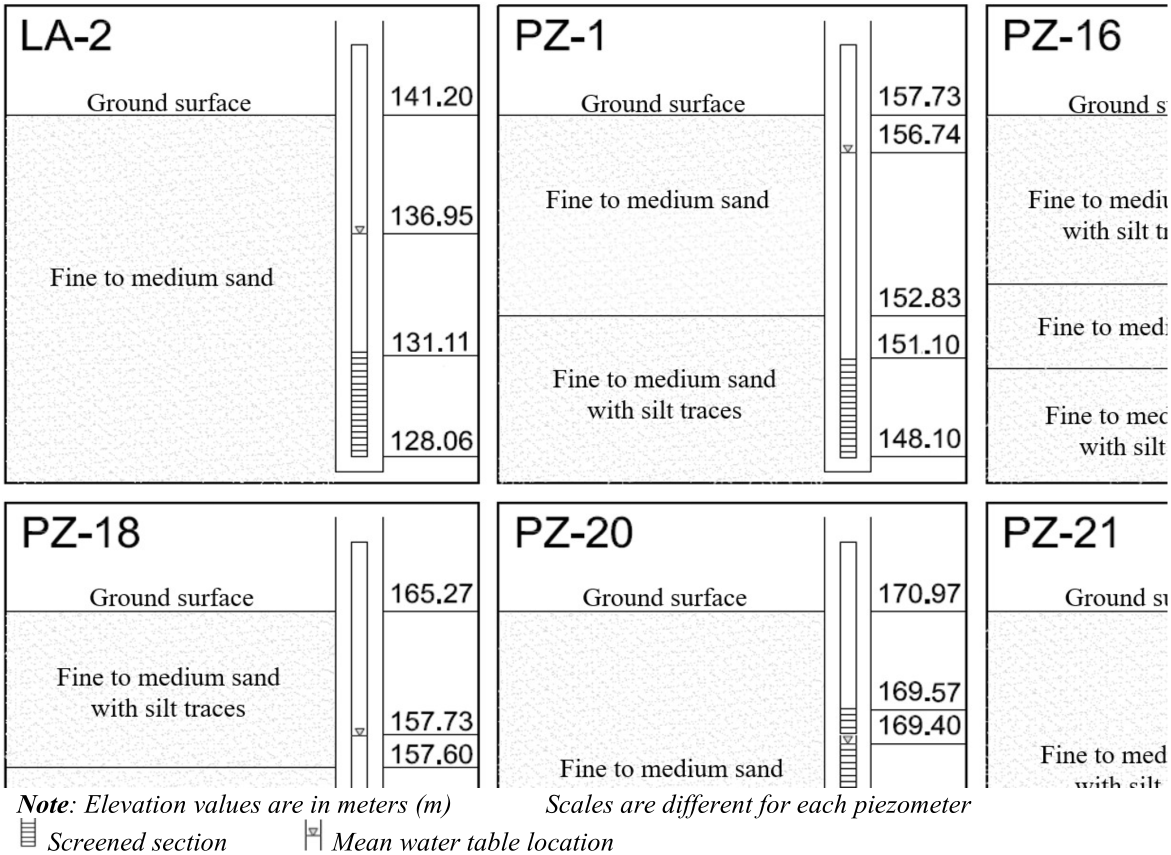


Figure 2. Stratigraphy and specific characteristics of the piezometers. Elevation values are expressed in meters above sea level "Adapted from Labrecque et al. (2020)".

### 2.2.2 *Vertical inflows*

Vertical input data was obtained from the Bagotville climate station, located 25 km away from the Saint-Honoré aquifer (Government of Canada, 2019). The change in the aquifer's water table level within the aquifer is assumed to be uniquely the result of the infiltrated amount of vertical inflow (snowmelt and rainfall). Water equivalent (in mm) originating from occasional or continuous snowmelt episodes is calculated from the daily thickness of lost snow (in cm). The ratio used for water equivalent conversion is the ubiquitous 10:1 which gives a value of 1 mm of water for 10 mm of snow on the ground (Potter, 1965). For example, on the day of 21 February 2017, the accumulated snow on the ground surface was recorded as 86 cm, whereas the next day, 22 February 2017, this value decreased to 84 cm. Thus, for 22 February 2017, a vertical input of 2 mm was considered. When only rainfall is captured during a given day, the considered daily vertical input is equivalent to the recorded rainfall amount (in mm). When rainfall and snowmelt occur simultaneously, a combined estimation of vertical inflows is calculated. Figure 3 shows the variation of the vertical inflows over 3 years (1 November 2014 to 8 December 2017), including the period covering the groundwater monitoring using the piezometers (the piezographs of piezometer PZ-18 are included as an example). The snow water equivalent calculated from the daily thickness of lost snow can lead to uncertainty concerning the amount of vertical inflow, because other natural processes such as sublimation could potentially contribute to reducing snow thickness on the ground surface without however contributing to the amount of water available for infiltration. For future research projects in comparable areas experiencing snowfall as meteorological input, it is strongly recommended to employ suitable methods for considering the sublimation effect.

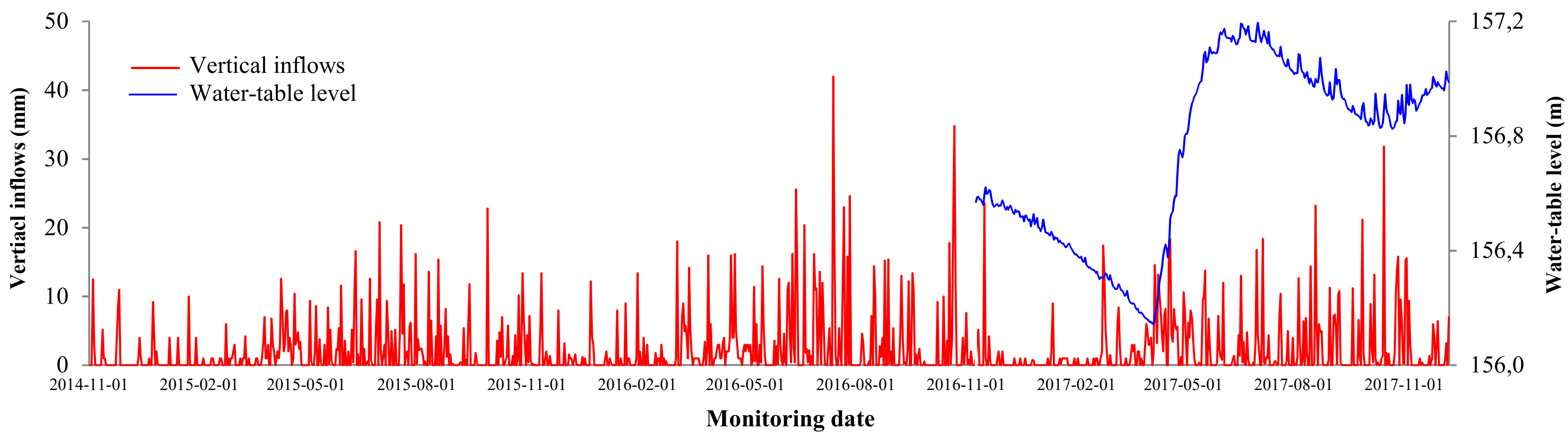


Figure 3. Vertical inflows and piezometric level at piezometer PZ-18 taken as example to show the groundwater monitoring period.

### 2.3 Correlogram method

#### 2.3.1 *Preliminary examination of time-series data*

A prior step was undertaken to visualize the overall time lag between the vertical inflows and the water table response, by plotting—together—the vertical inflows and the water table level time-series data. As those times-series data have shown detectable frequency variations (Figure 3), as a first step, their subsets were adjusted by smoothing out the original time-series data using a simple 15-day moving average to decrease the detectable frequency variations. Secondly, the adjusted time-series data were normalized by subtracting the mean and dividing the result by the standard deviation. Figure 4a shows the normalized vertical inflow and water table level data for piezometer PZ-18, provided as an example. Figure 4b shows the period in which the two sets of normalized time-series data have similar shapes, and are separated by a distinct time period, indicating that the water table level is responding to the vertical inflow after a certain time lag. For example, from Figure 4b: time lag (1) = 105 days, (2) = 71 days, and (3) = 128 days ($\simeq$ 4 months); this last appears to be the longest time lag. Hence, the correlogram process should consider a period for the vertical inflow events starting at least 4 months before the first day of the water table level monitoring. A period of 5 months is considered in the present study (see Figure 5a).

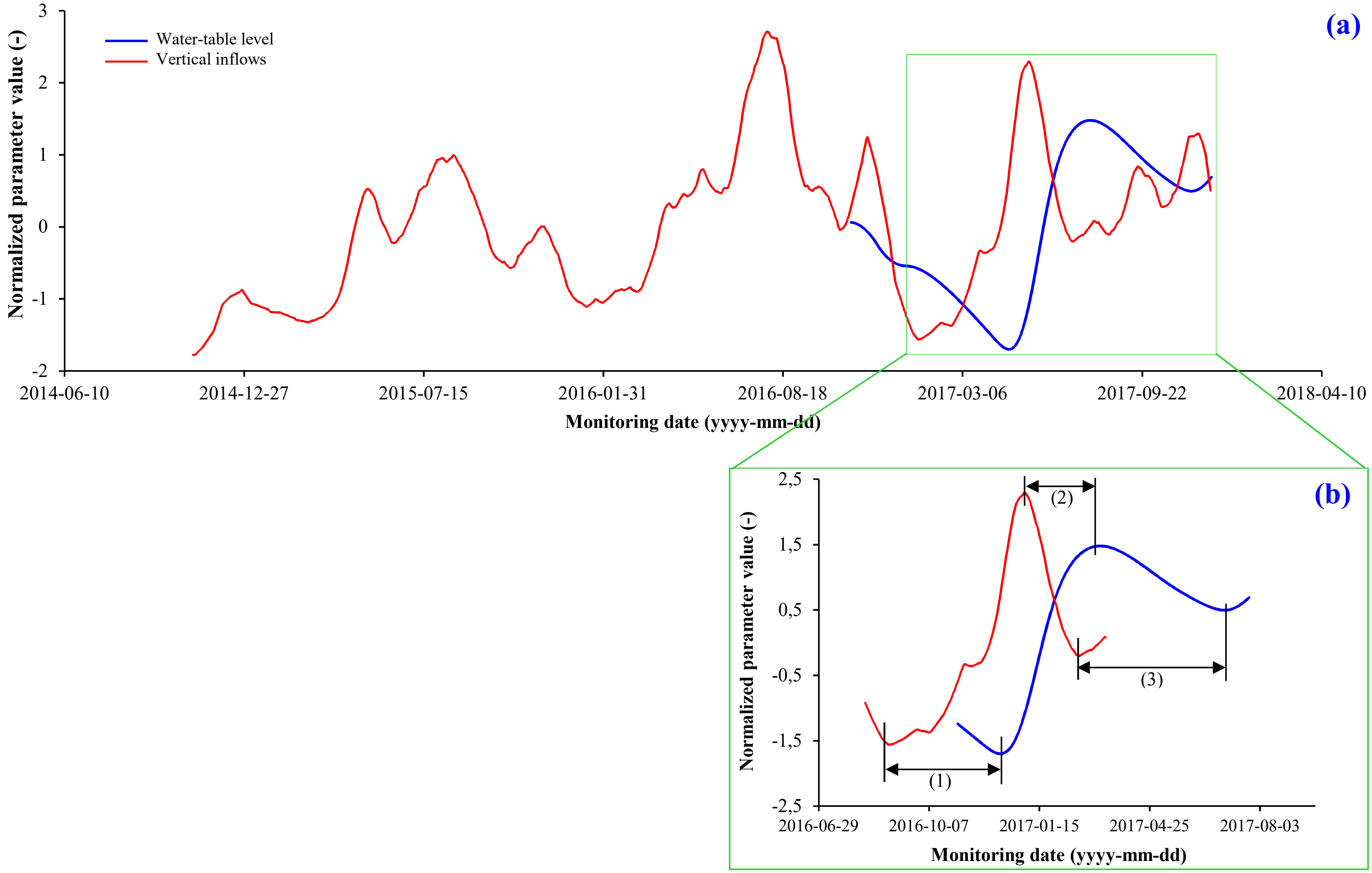


Figure 4. (a) Normalized vertical inflows and water-table levels from the monitored piezometer PZ-18 (the vertical inflows and water-table level time-series data were normalized by subtracting the mean and dividing the result by the standard deviation); (b) Zoom on the period during which the two normalized time-series of data have an approximately similar shape; in Figure 4b, (1), (2) and (3) are time-lag lasting (1) = 105 days, (2) = 71 days, and (3) = 128 days (≃ 4 months).

### 2.3.2 *Cross-correlation*

The cross-correlation function can be used to determine the relationship between two time-series when one of them is delayed in time with respect to the other (in this case, water table fluctuations occur after vertical inflows). The cross-correlation data processing produces a curve representing a continuous series of similarity evaluations, in which the peak of this curve occurs at a time lag for which the two time-series are best correlated, in other words, most similar (Box et al., 1994). In the case of water table fluctuations relative to vertical inflow, the cross-correlation peak corresponds to the time lag defining the aquifer response time (Delbart et al., 2014). Mathematically, the cross-correlation function is solved as follows:

$$r_{xy}(k) = \frac{C_{xy(k)}}{\sigma_x \sigma_y} \quad (1)$$

where, $r_{xy}(k)$ is the cross-correlation function, $C_{xy}(k)$ is the cross-correlogram (Equation 2), $\sigma_x$ and $\sigma_y$ are the standard deviations of the two $x$ and $y$ time-series.

$$C_{xy}(k) = \frac{1}{n} \sum_{t=1}^{n-k} (x_t - \bar{x}) (y_{t+k} - \bar{y}) \quad (2)$$

where $k$ is the time interval between the finite time-series limited by $n$, $n$ is the length of the time-series, $x_t$ and $y_t$ are respectively the input and output time-series, $\bar{x}$ and $\bar{y}$ are respectively the input and output average time-series.

### 2.3.3 *Sliding cross-correlation method*

The aquifer's response time was assessed using the sliding cross-correlogram method (Delbart et al., 2014). An illustration of the cross-correlogram processing conducted in the present study is shown in Figure 5. The method consists in selecting a period in the time-series data for the water table level (fixed-window) and determining the location of a similar period in the time-series data for the vertical inflows (sliding-window). The process of selecting a ‘‘fixed-window’’ from the water-table fluctuations time series data and a ‘‘sliding-window’’ from the vertical-inflows time series data does not imply that the water table level is impacting the vertical inflow according to a certain time lag. Processing starts by correlating the first fixed-window with the first sliding-window (the first window starts at the beginning of the time-series data - Figure 5a). This processing aims to mathematically evaluate the degree of similarity between the two correlated windows; this evaluation produces a correlation coefficient value. The fixed-window is maintained in position at the beginning of the time-series data, while sliding of the sliding-window is gradually performed through the entire time-series data according to a defined sliding-time interval. In the present study, the sliding-time interval is 20 days (Figure 5a) to follow the gradual seasonal variation over time of the vertical inflows and water table fluctuations. Cross-correlation provides a series of correlation coefficients that can be illustrated as a cross-correlation function curve (Figure 5b), wherein the peak occurs at a time lag for which the fixed and sliding-window time-series data are highly similar. This time lag represents the aquifer response time. A single cross-correlation function curve may present several peaks, however, and as practiced by Delbart et al. (2014), only the first correlation peak is considered in the present study. For a cross-correlation to be acceptable, the correlating process result must attain a significant degree of confidence (95% confidence level); i.e., the correlation coefficient *r(k)* corresponding to the peak value must be superior to the standard error determined as $2/N^{1/2}$, where $N$ is the number of values in the data set (Diggle, 1990). A similar significance test has been used in similar studies to determine the acceptability of cross-correlation coefficients (Chiaudani et al., 2017; Delbart et al., 2014; Duvert et al., 2015; Lee et al., 2006).

In this study, several cross-correlation processing attempts were put to the test using different time-windows (90, 100, 110 days, etc.); the acceptable correlation coefficient values observed in the present study were obtained based on a time-window of 160 days. When the cross-correlogram obtained with the first fixed-window was completed (Figure 5b), the same process was repeated with a second fixed-window, by sliding from the first fixed-window according to a defined sliding time-interval of 20 days (Figure 5a). Again, this sliding time-interval is considered to follow the gradual seasonal variation over time of the vertical inflows and water table fluctuations. Another cross-correlation function curve is then produced (Figure 5c) and so on (see another example in Figure 5d). The cross-correlation values were processed using a codified-automated program implemented in MATLAB R2018a. An example of the compiled results representing the aquifer response times (ART) is shown in Figure 5e. In Figure 5e for instance, the ART10 is assessed to be 74 days, i.e., the vertical inflow event that occurred on 16 February 2017 reached the water table on 1 May 2017 (after a travel time of 74 days through the subsurface). 1 May 2017 is the first day of the relative fixed-window and the aquifer response time is considered to be representative of the first vertical inflow date. This date is determined by subtracting the determined time lag (the aquifer response time) from the first day of the relative fixed-window.

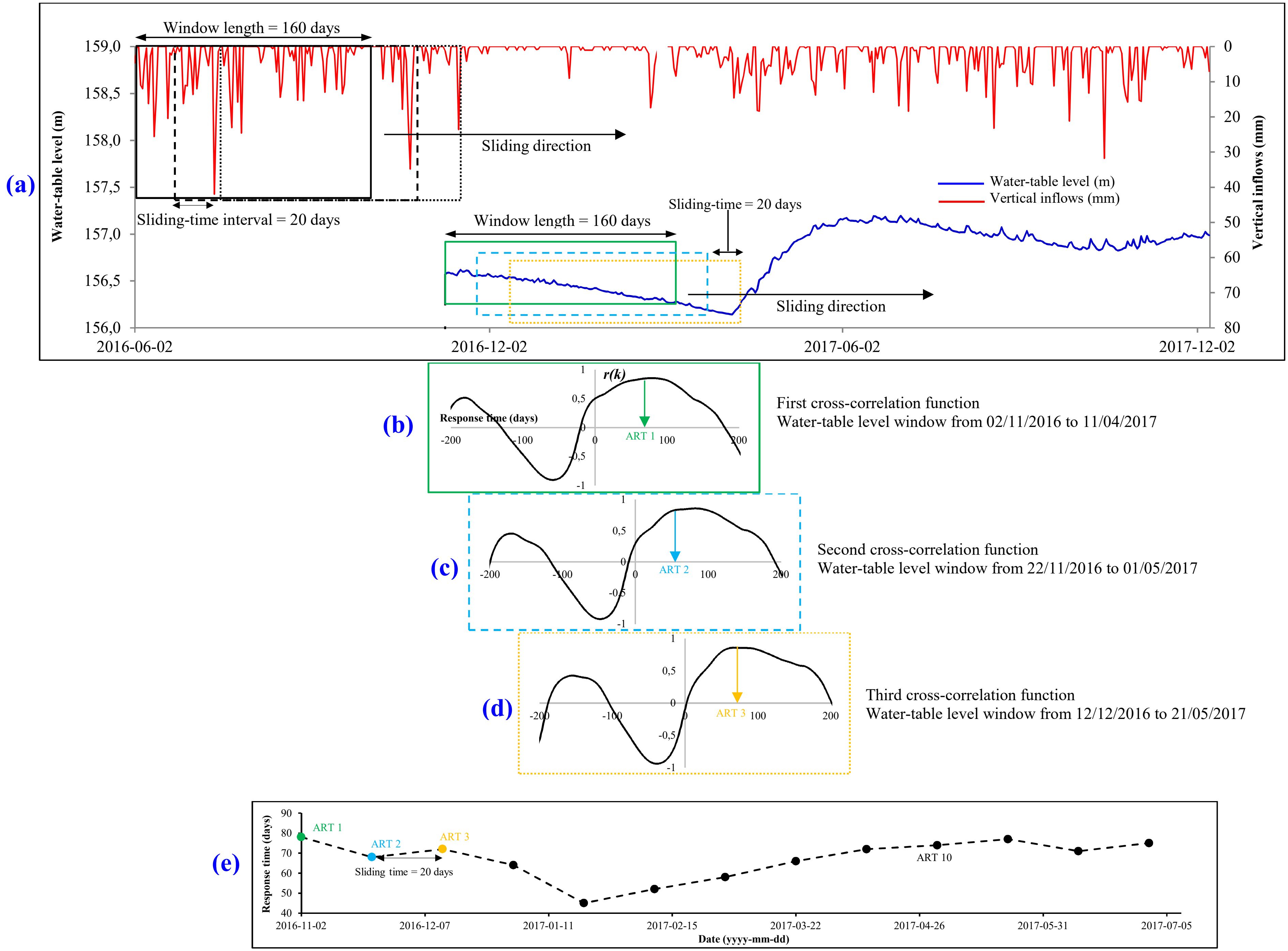

(a)
Window length = 160 days
Sliding direction
Sliding-time interval = 20 days
Window length = 160 days
Sliding-time = 20 days
Sliding direction
Water-table level (m)
Vertical inflows (mm)
159,0
158,5
158,0
157,5
157,0
156,5
156,0
0
10
20
30
40
50
60
70
80
2016-06-02
2016-12-02
2017-06-02
2017-12-02
(b)
r(k)
Response time (days)
ART 1
First cross-correlation function
Water-table level window from 02/11/2016 to 11/04/2017
(c)
ART 2
Second cross-correlation function
Water-table level window from 22/11/2016 to 01/05/2017
(d)
ART 3
Third cross-correlation function
Water-table level window from 12/12/2016 to 21/05/2017
(e)
Response time (days)
ART 1
ART 2
ART 3
Sliding time = 20 days
ART 10
Date (yyyy-mm-dd)
2016-11-02
2016-12-07
2017-01-11
2017-02-15
2017-03-22
2017-04-26
2017-05-31
2017-07-05

Figure 5. Principle of the sliding cross-correlogram method used in the present study. This principle is adapted from Delbart et al. (2014); however, the graphics, dates and other information shown in these figures represent data from the present study: (a) represents the time-series data of vertical inflows and the water table level; (b) shows a part of the cross-correlation functions curve relating to the first correlogram processing. The peak corresponds to the first determined aquifer response time (ART); (c) and (d) are the subsequent cross cross-correlation functions; (e) is the compilation of the response times assessed from the cross-correlation functions.

## 3 Results and discussions

### 3.1 Vertical inflows and water table level time-series

The calculated vertical inflows, representing the amount of water available for infiltration over the considered period (2 June 2016 to 8 December 2017), are shown in Figure 6a. Intense rainy events occurred during the summer and autumn seasons, during which considerable vertical inflows were expected. Large amounts of water are also expected during the snowmelt period, generally occurring in the mid-spring season (April), when 4–5 months of accumulated snowpack is rapidly transformed into water available for infiltration. Figure 6a shows that only limited water amounts are available for infiltration during the period when snow covers the land. During this period, cold conditions greatly limit the recharge of the aquifer. Nonetheless, occasional snow melt—occurring as a response to occasional increases in temperature—have generated minor amounts of water available for infiltration, as can be observed in Figure 6a. The daily water table levels at the six monitored piezometers (LA-2, PZ-1, PZ-16, PZ-18, PZ-20 and PZ-21) have shown different variation intervals (Table 1). Significant seasonal variations of the water table level are distinguishable—for all the monitored piezometers—featuring periods showing high water table levels (summer-autumn seasons) interspersed with periods of lower water table levels (winter-spring seasons). All six monitored piezometers produced generally similar patterns, suggesting that the study area captures precipitation according to a generally uniform distribution pattern. However, as can be seen in Figure 6b and Table 1, there are certain discernible differences in water table levels between the monitored piezometers; such differences may be related to piezometer-site characteristics, including surface and bedrock leveling.

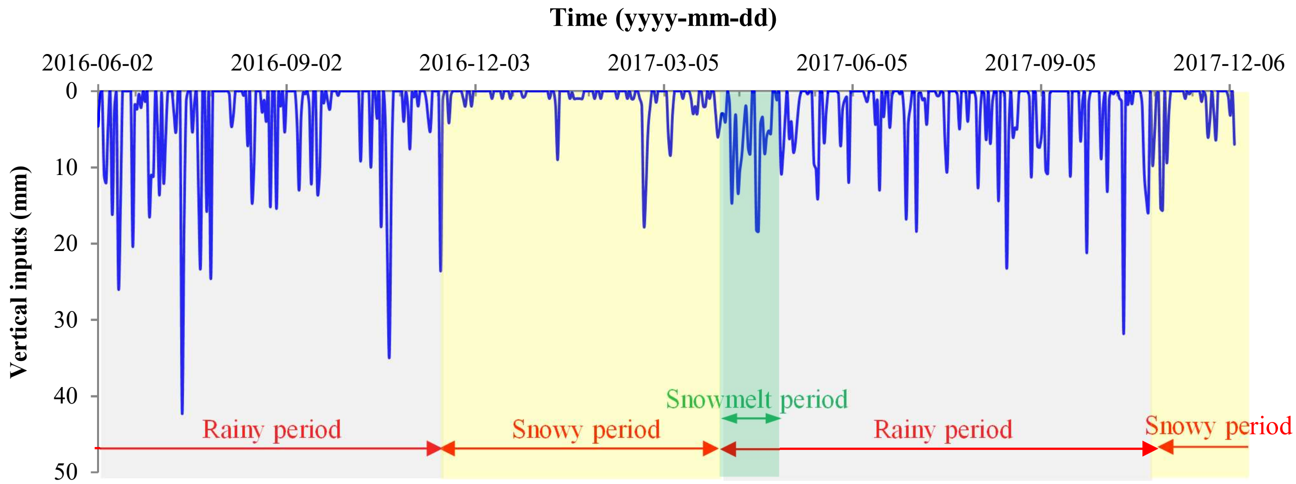


(a)

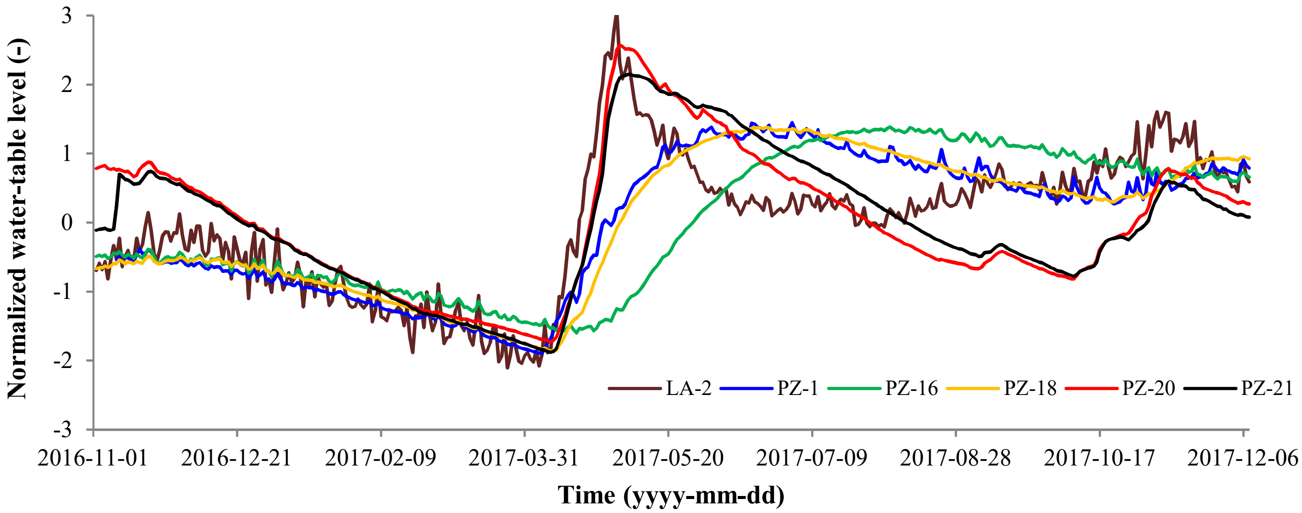


(b)

Figure 6. (a) Variation of the vertical inflows considered in the present study; (b) Normalized piezometric level of time-series data obtained from the monitored piezometers.

Table 1. Water-table measurements at the monitored piezometers.

| | Piezometer | | | | | |
|---|---|---|---|---|---|---|
| **Measurements (m)** | **LA-2** | **PZ-1** | **PZ-16** | **PZ-18** | **PZ-20** | **PZ-21** |
| Highest water-table level (m a.s.l.) | 136.85 | 156.14 | 146.43 | 157.10 | 168.85 | 168.74 |
| Lowest water-table level (m a.s.l.) | 137.11 | 157.20 | 147.05 | 158.19 | 170.23 | 169.88 |
| Variation range of water-table (m) | 0.26 | 1.05 | 0.62 | 1.09 | 1.38 | 1.14 |

*a.s.l. = above sea level*

### 3.2 Assessed aquifer response time

Using a sliding window of 160 days and a sliding interval of 20 days over the entire water table level time-series (from 2 November 2016 to 8 December 2017), 13 sliding-window cross-correlogram functions were generated for each monitored piezometer excepting PZ-1. For the latter, 12 rather than 13 sliding-window cross-correlogram functions were generated, because at this piezometer, measurements of the water table level were taken starting on 9 November 2016 rather than on 2 November 2016, as was the case for all the other piezometers. The number of values in each data set ($N$) is 160 because the considered windows are for 160 days; thus, the calculated standard error value ($2/N^{1/2}$) is 0.16. Through cross-correlogram processing, all the first peaks of the correlation coefficient $r(k)$ are found to be significant with standard error values greater than 0.16 (see illustrative examples in Figures 5b, c and d showing $r(k)$ greater than 0.16). The aquifer response times obtained at the six monitored piezometers are presented in Figure 7, which shows that each piezometer exhibited specific and different aquifer response times compared to the other piezometers. The different aquifer response times obtained from the six monitored piezometers in the same aquifer indicate that the hydraulic behavior at each piezometer is related to specific highly localized site effects, potentially controlled by aquifer characteristics that appear to be different from one location (piezometer) to another. We investigated the available specific characteristics observed at the site of each of the piezometers thought to explain the observed differences in the aquifer response times (Table 2).

Table 2. Site characteristics at the monitored piezometers.

| | Piezometer | | | | | |
|---|---|---|---|---|---|---|
| **Site characteristics** | **PZ-16** | **PZ-18** | **PZ-1** | **PZ-21** | **PZ-20** | **LA-2** |
| Minimum response time (days) | 63 | 45 | 35 | 39 | 34 | 18 |
| Maximum response time (days) | 116 | 78 | 70 | 61 | 59 | 56 |
| Mean response time (days) | 91 | 67 | 58 | 46 | 41 | 31 |
| Mean vadose zone thickness (m) | 13.28 | 7.70 | 1.20 | 1.38 | 1.63 | 4.25 |
| Mean vertical inflow intensity (mm/d) | 1.44 | 1.73 | 2.07 | 2.35 | 2.33 | 2.21 |
| Mean local recharge (mm/day)[1] | 0.51 | 0.95 | 1.22 | 1.23 | 1.33 | 0.45 |
| Subsurface material | FMSTS | FMSTS | FMSTS | FMSTS | FMSTS | FMSTS |

*1: Data were obtained from Labrecque et al. (2020)*
*FMSTS: Fine to medium sand with some traces of silt (Figure 2)*

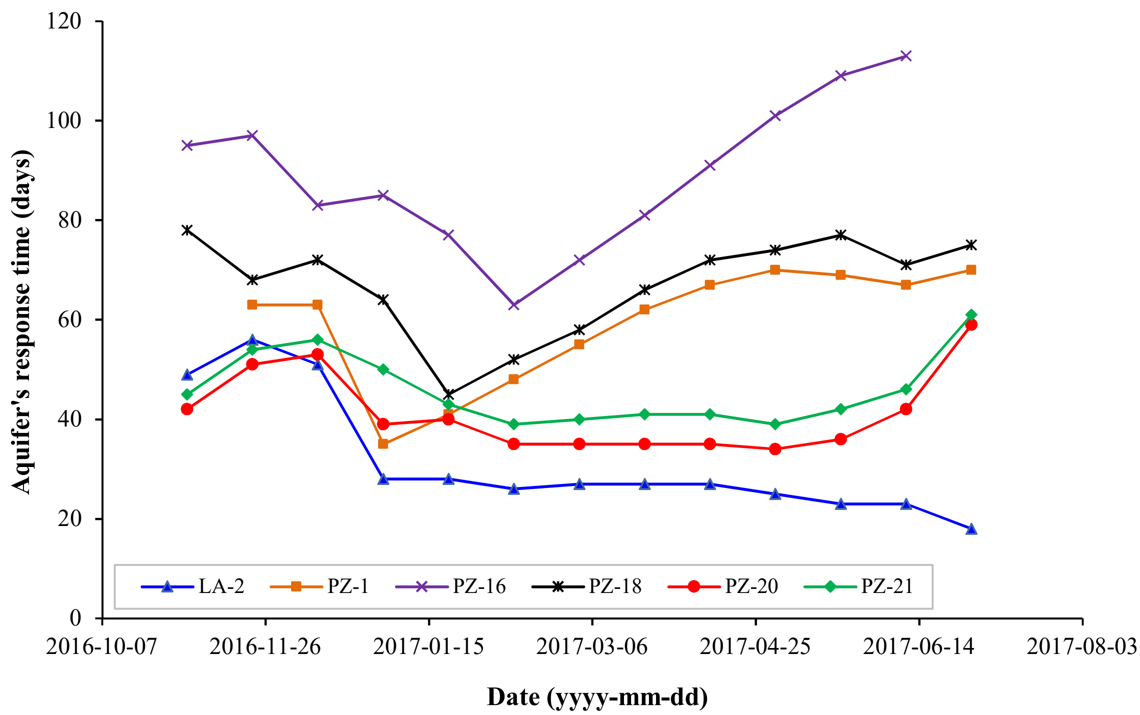


Figure 7. Aquifer response times assessed at the six monitored piezometers.

The longest mean aquifer response time of 91 days observed for PZ-16 is associated with the greatest mean thickness of the vadose zone at 13.28 m. This observation illustrates the usual positive relationship between the aquifer response time and the thickness of the vadose zone; i.e., when the thickness increases, the response time increases (Lee et al., 2006). However, PZ-1 presenting the thinnest mean vadose zone of 1.2 m (Table 2) exhibits a longer mean aquifer response time of 58 days, compared to other piezometers that exhibit a relatively thick mean vadose zone such as PZ-20, PZ-21 and LA-2 (Table 2). Furthermore, piezometer LA-2, with a mean vadose zone (4.25 m) thicker than that of PZ-20 (1.63 m), shows a shorter mean aquifer response time (31 days) compared to that of PZ-20 (41 days). Accordingly, it can be deduced that the thickness of the vadose zone is not the main site characteristic influencing the observed differences in aquifer response times between the monitored piezometers of the study area. When considering 4 of the 6 piezometers PZ-16, PZ-18, PZ-1, and PZ-21 (Table 2), a clear relationship is observed between the vertical inflow intensity and the aquifer response time: when the vertical inflow intensity increases, the aquifer response time decreases. This observation could be related to the soil unsaturated hydraulic conductivity because the infiltrated water contributes soil volumetric water content above the water table, leading to higher soil unsaturated hydraulic conductivity. However, the vertical inflow intensity cannot exert a significant effect on the aquifer response time when the captured precipitation, even if intense, is totally or partially lost via possible runoff and/or evapotranspiration. For this reason, the soil unsaturated hydraulic conductivity, which potentially controls the aquifer response time, is mostly affected by the amount of the water available for infiltration (recharge). Table 2 shows the mean local recharge rate at the monitored piezometer sites, wherein the observed difference in recharge can be associated with site effects, such as runoff process and topography (Chesnaux and Stumpp, 2018; Labrecque et al., 2020). When 5 monitored piezometers PZ-16, PZ-18, PZ-1, PZ-21, and PZ-20 are considered in Table 2, a direct proportional inverse relationship between the mean local recharge and the mean aquifer response time is observed: when the mean local recharge increases, the mean aquifer response time decreases. Hence, the effect of recharge on the aquifer response time can be confirmed. In this study, the intense recharge combined with the higher soil unsaturated hydraulic conductivity create a cumulative effect leading to shorter aquifer response times. The potential effect of differences in subsurface material on the aquifer response times is not considered in the present study because all the monitored piezometers are surrounded by similar geological material, mostly dominated by fine to medium sand with some traces of silt (Figure 2). The numerical modeling of groundwater flow through the vadose zone can be used to verify the assumptions related to the factors influencing the aquifer response time—including the vertical distribution of the unsaturated hydraulic conductivity—but such numerical modeling would require an intense and continuous technical fieldwork monitoring data of the entire thickness of the vadose zone (Hopmans et al., 2002; Konikow, 2011; Vereecken et al., 2016; Vero et al., 2017), which is outside the scope of the present study.

As observed in Figure 7, the aquifer response time is generally variable over the study period for all the monitored piezometers; in addition, each piezometer shows different aquifer response times. However, the similarity in shape between the response time trends (Figure 7) suggests a generally similar influence of seasonal conditions. PZ-18 was the only piezometer monitored in this study to be located in an urbanized area; the other monitored piezometers were located mainly within forested areas. Despite this, PZ-18 did not display distinctly different aquifer response times from the others: the longest mean aquifer response time (91 days) was observed for PZ-16, while the shortest mean aquifer response time (31 days) was found for LA-2. It should be noted that urbanization may slow down the natural recharge of aquifers, due to ground surface sealing by concrete and asphalt cover (Baier et al., 2014). Waterproofing due to ground sealing could affect the spatial and deep distribution of groundwater, compounded by the conversion of precipitation into runoff rather than infiltration into the aquifer (Wakode et al., 2018). Although the area surrounding PZ-18 is documented as urbanized, it contains only the local airport of Saint-Honoré with its short landing runways as well as several small-scale associated buildings. Hence, in effect, the PZ-18 sector is not densely urbanized, and consequently, the effect of urbanization on aquifer response times at PZ-18 was found to be insignificant.

PZ-1 shows a mean response time of 58 days over a vadose zone thickness of 1.2 m. This means that at the PZ-1 site, infiltrating water takes approximately 1 year to travel 7 m through the vadose zone. This result was confirmed in other studies by using stable isotope-based method (Boumaiza et al., 2020b) and numerical modeling (Boumaiza et al., 2020a) at an investigated site located 100 m from PZ-1. These findings support the outcomes of the present study. In Figure 7 the piezometers show a decreasing trend of the aquifer response times (from longer to shorter) over the winter period (overall from November to March - Figure 7), before increasing from early spring to late summer (overall from March to July - Figure 7). This means that the shorter aquifer responses times generally occurred during the winter-season, whereas the longer aquifer responses times occurred during the summer season. Aquifer response times were found to be shorter during periods of high water table levels and longer during periods of low water table levels (Larocque et al., 1998; Lee et al., 2006). In this northern study area, however, the winter season is known to be associated with lower water table levels, due to limited water amounts available for infiltration (because of snowpack cover); while the summer season is known to be associated with higher water table levels (because of high amounts of infiltrated water originating from snowmelt episodes during the Spring season and rain events occurring during the summer season). The observation in the present study which is contrary to the norm—(the norm is shorter response times during the low-depth of water table level period and longer response times during the high-depth of water table level period)—is explained by the long duration of the aquifer response time. In fact, all the monitored piezometers reveal a relatively long mean aquifer response time, with a mean magnitude ranging from 31 to 91 days (Table 2). Aquifer response times up to 110 days have been measured in alluvial aquifers (Duvert et al., 2015), whereas in fractured-rock aquifers, much shorter mean response times of 17 hours have been determined by Larocque et al. (1998). Let us compare the hydraulic behavior of fractured-rock aquifers against that of alluvial aquifers. In fractured-rock aquifers experiencing shorter response times, the captured rainfall quickly reaches the water table. For this reason, there is a general inverse relationship between the aquifer response time and the water table level; when one increases, the other diminishes, and vice versa. However, this inverse relationship cannot be rapidly observed in granular aquifers by reason of the inherent longer response times. In the case of our granular aquifer, to plot this inverse relationship between the aquifer response time and the water table level, the water table level should be considered at the time corresponding to the date of occurrence of the vertical inflow, rather than the moment when the water table reacts to the vertical inflow event. This is considered for linking the water table level to the moment corresponding to the date of occurrence of the vertical inflow. For example, the aquifer's first response time for PZ-21 is determined to be 45 days (Figure 7); the water table level corresponding to this aquifer response time is the level that existed 45 days before the date of the beginning of the first fixed-time window, i.e., 2 November 2016 (we consider the first fixed time-window because the given example is for the aquifer's first response time). Even though the available water table monitoring data does not cover the period before 2 November 2016, we may nonetheless regard the yearly water table monitoring data (2016/2017) as representative of yearly fluctuations in the local water table. The error associated with this assumption is expected to be minimal, as seasonal climate characteristics have not experienced significant changes over the monitored year 2016/2017 or the previous year 2015/2016, as can be observed in Figure 4a.

Figure 8 shows the determined (back-tracked) water table levels and the corresponding aquifer response times for all the monitored piezometers, in which an inverse relationship between the water table level and the aquifer response time is generally observed: when one increases, the other diminishes, and vice versa. Delbart et al. (2014) found that fractured-rock aquifer response times are shorter during the summer, while Larocque et al. (1998) who also studied a fractured-rock aquifer, as well as Lee et al. (2006) who investigated a chalk aquifer (soft fractured limestone) found that aquifer response times are shorter in wet seasons than in dry seasons ("dry seasons" are usually summer and autumn). Imagawa et al. (2013) also assessed the aquifer response times in an alluvial aquifer according to three contrasting climate patterns. They established that response times in dry conditions were at least twice longer than during wet periods of elevated rainfall. Larocque et al. (1998) explained that the saturation of the aquifer's fracture network during the wet seasons allows a more rapid transmission of the water pulse, compared to dry seasons where the aquifer's fracture network is unsaturated, and consequently, the water pulse is transmitted more slowly. During the wet seasons, Lee et al. (2006) observed a high water table level in the chalk aquifer they studied, with a thinner vadose zone compared to dry seasons. These authors established a direct positive proportional relationship between the aquifer response times and the thickness of the vadose zone. A similar relationship was observed in the present study. Figure 8 shows the relationship between the aquifer response time and the water table level; as the water table level increases, the vadose zone diminishes; inversely, when the water table is lower, an increase of the vadose zone is observed. There is general agreement concerning the existence of a direct positive relationship between aquifer response times and vadose zone thickness, i.e., shorter response times are observed when the water table level rises and the vadose zone decreases, and vice versa (Figure 8). This observation is potentially related to the unsaturated hydraulic conductivity. In fact, a thinner vadose zone induces a shorter response time because a shallow water table yields a higher soil volumetric water content above it—close to the soil saturated value—leading to a higher unsaturated hydraulic conductivity. Inversely, a thicker vadose zone causes a longer aquifer response time, because a deeper water table yields lower soil saturated values, leading to low values of unsaturated hydraulic conductivity. The effect of vadose zone saturation on aquifer response times has been mentioned by Delbart et al. (2014), who showed that variations in response times are more likely due to variability of the transfer velocity within the vadose zone. This transfer velocity depends on the saturation of the vadose zone's fracture network. The saturation of the fractured-rock aquifer was observed to be linked to higher rainfall intensity, explaining the observed shorter response time of the aquifer. For the alluvial system investigated in the present study, Figure 9—showing the intensity of vertical inflows and the corresponding response times of the aquifer at the monitored piezometers—confirms the inverse relationship that exists between the intensity of the vertical inflows and the aquifer response times. It was generally observed for the six monitored piezometers that when the vertical inflow increases, the aquifer response times decreased (Figure 9).

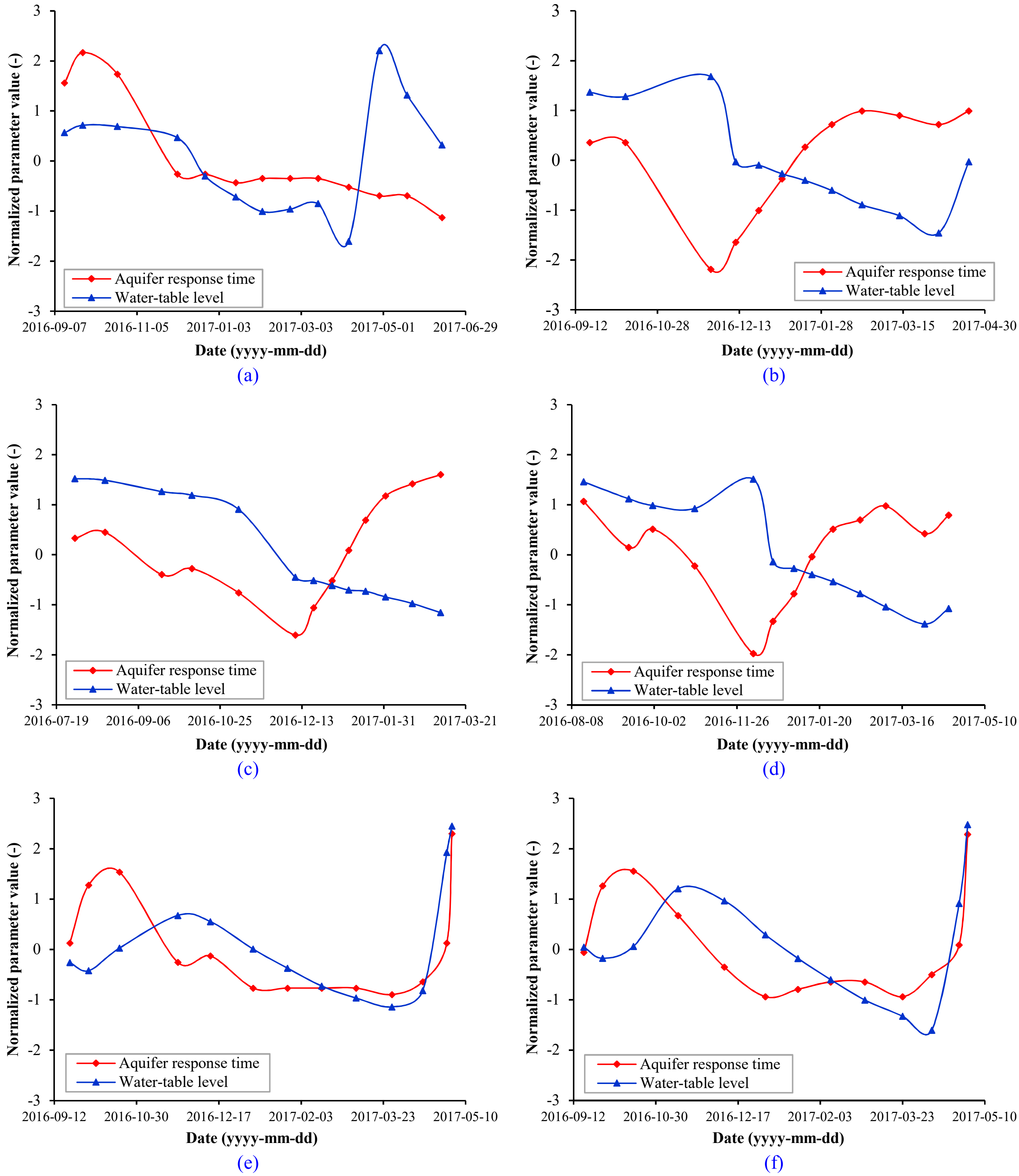


Figure 8. Back-tracked water-table levels and the corresponding aquifer's responses time (both normalized using standard scores, i.e., by subtracting the mean and then dividing the result by the standard deviation) at piezometers (a) LA-2, (b) PZ-1, (c) PZ-16, (d) PZ-18, (e) PZ-20, (f) PZ-21. Dates correspond to the back-tracked dates considering the determined time-lag from Figure 7.

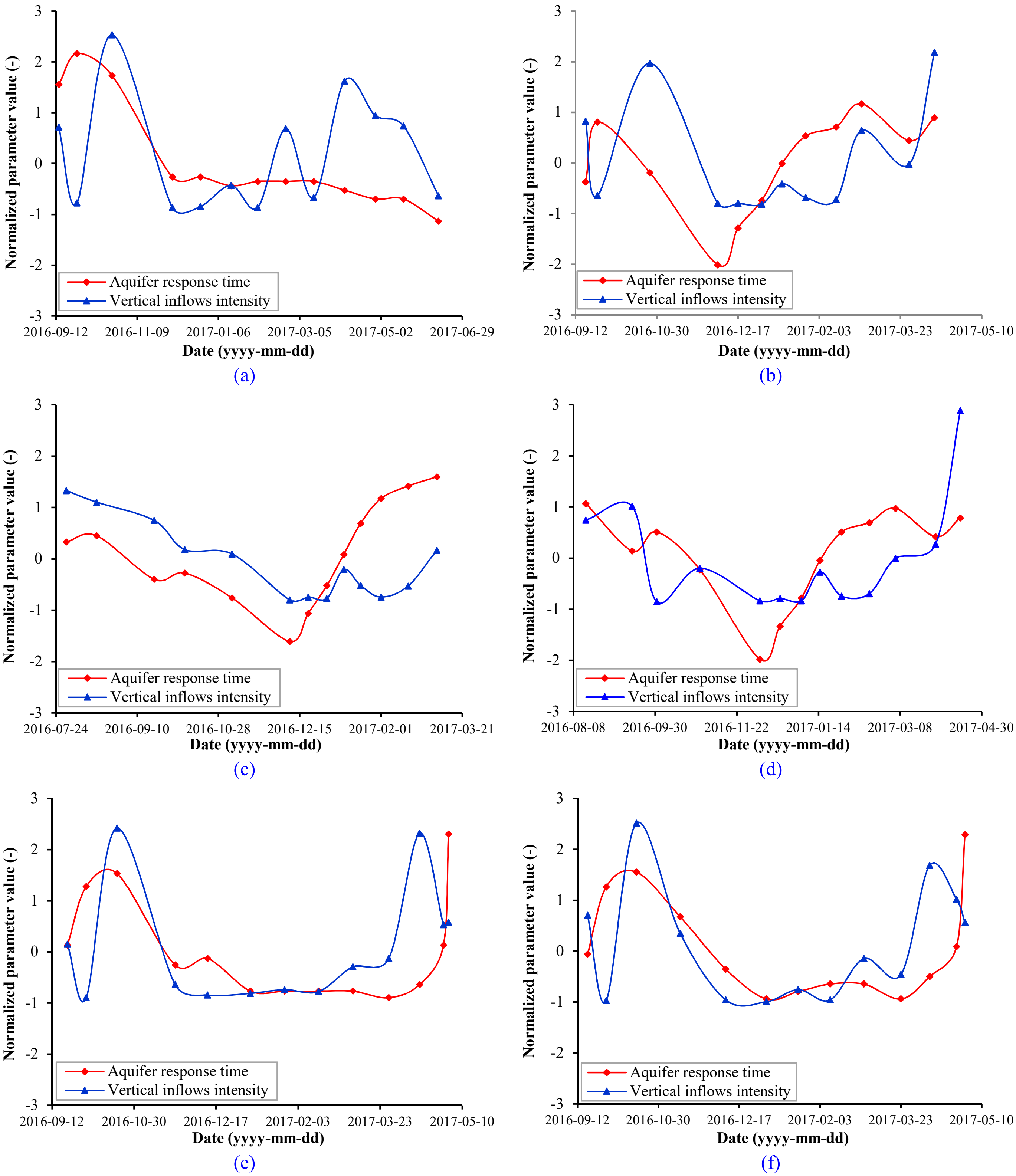


Figure 9. Back-track analysis of vertical inflow intensity and the corresponding aquifer response times (both normalized using standard scores, i.e., by subtracting the mean and then dividing the result by the standard deviation) at piezometers (a) LA-2, (b) PZ-1, (c) PZ-16, (d) PZ-18, (e) PZ-20, (f) PZ-21. The dates correspond to the back-tracked dates considering the time-lag determined from Figure 7.

## 4 Conclusions

The case study research reported in the present study is based on the analysis of aquifer response time over an alluvial aquifer subject to variations of meteorological inputs over time. Analysis of correlations was conducted between the amount of vertical inflows available for infiltration and water table levels, to determine the aquifer response time. The present study demonstrates that the sliding cross-correlogram approach provides a useful analysis for assessing the spatiotemporal distribution of the response times of an alluvial aquifer, and for investigating the impact of aquifer characteristics on these response times. The aquifer response times obtained at the six monitored piezometers showed that each piezometer exhibited specific and different aquifer response times compared to the other piezometers. Spatiotemporal variability of aquifer response times over the study area were observed, with mean aquifer response times varying from 31 to 91 days. This study highlights not only the seasonal variation of aquifer response times in the study area, but it also indicates, based on the observed differences in aquifer response times in different sectors of the same aquifer, that it would be erroneous to assume that a single aquifer must always exhibit the same hydraulic behavior at its different studied locations. The results obtained in the present study further highlight the known relationships between aquifer response times and site characteristics; shorter aquifer response times are related to the rise of the water table level, and subsequently, to the variations over time of the vadose zone thickness. A further observation is that aquifer response times are often observed to be linked to the vertical inflow intensity; when vertical inflow intensity increases, aquifer response times decrease. This observation is potentially related to the soil unsaturated hydraulic conductivity, as the infiltrated water contributes soil volumetric water content above the water table; this process subsequently leads to higher soil unsaturated hydraulic conductivity.

As the hydraulic conductivity is also impacted by the amount of water available for infiltration, an inverse relationship is observed in the present study between the aquifer response times and the local recharge rate: when the local recharge rate increases, the aquifer response times decrease. Hence, the effects of the soil unsaturated hydraulic conductivity are combined with that of recharge (a cumulative effect). The geological history of the SLSJ region has given rise to several hydrogeological systems which produce abundant drinking water of high quality; therefore, the framework followed in the present study can be usefully applied to those aquifers which are under similar climate conditions. Assessing the spatiotemporal distribution of the aquifer response times and understanding the effect of aquifer properties on aquifer response times can support the decision of whether to explicitly consider the effect of site characteristics on the time lag between precipitation and water table fluctuations. In the present study, only a portion of the Saint-Honoré aquifer was considered for investigation, as the monitored piezometers are appropriately distributed over this portion. However, additional piezometers are recommended to be installed over the entire area of the Saint-Honoré aquifer to gain a comprehensive understanding concerning the distribution of aquifer response times. Any future implementation of additional piezometers in the investigated aquifer should include a plan to sample continuous vertical sediment cores, in order to estimate the hydraulic properties of the main geological units affecting the vertical water flow. This would contribute valuable information to the study and interpretation of aquifer response times.

**Acknowledgments:**

The authors would like to thank the Natural Sciences and Engineering Research Council of Canada for funding this project (Grant Nr. RGPIN-2020-04721). The authors would like to thank Mr. David Noël for his much-appreciated technical fieldwork. In addition, the authors wish to thank the well owners (Mr. Christian Bouchard and Mr. Dany Gauthier), who graciously provided free access to their piezometers. Dr. Célestine Delbart from University of Tours (France) is tanked for her valuable explanations and helps. Ms. Josée Kaufmann is thanked for editorial collaboration.

## References

Allocca, V., De Vita, P., Manna, F., Nimmo, J.R., 2015. Groundwater recharge assessment at local and episodic scale in a soil mantled perched karst aquifer in southern Italy. Journal of Hydrology 529, 843–853.

Baier, K., Schmitz, K.S., Azzam, R., Strohschoen, R., 2014. Management Tools for Sustainable Ground Water Protection in Mega Urban Areas-Small Scale Land use and Ground Water Vulnerability Analyses in Guangzhou, China. International Journal of Environmental Research 8, 249–262.

Bailly-Comte, V., Jourde, H., Roesch, A., Pistre, S., Batiot-Guilhe, C., 2008. Time series analyses for Karst/River interactions assessment: Case of the Coulazou river (southern France). Journal of Hydrology 349, 98–114.

Bouchaou, L., Mangin, A., Chauve, P., 2002. Turbidity mechanism of water from a karstic spring: Example of the Ain Asserdoune spring (Beni Mellal Atlas, Morocco). Journal of Hydrology 265, 34–42.

Boumaiza, L., 2008. Caractérisation hydrogéologique des hydrofaciès dans le paléodelta de la rivière Valin au Saguenay [Hydrogeological characterization of hydrofacies in the Valin River Paleodelta in Saguenay]. Master's Thesis, Université du Québec à Chicoutimi, Québec, Canada.

Boumaiza, L., Chesnaux, R., Walter, J., Stumpp, C., 2020a. Constraining a flow model with field measurements to assess water transit time through a vadose zone. Groundwater. https://doi.org/doi.org/10.1111/gwat.13056

Boumaiza, L., Chesnaux, R., Walter, J., Stumpp, C., 2020b. Assessing groundwater recharge and transpiration in a humid northern region dominated by snowmelt using vadose-zone depth profiles. Hydrogeology Journal 28, 2315–2329.

Boumaiza, L., Rouleau, A., Cousineau, P.A., 2019. Combining shallow hydrogeological characterization with borehole data for determining hydrofacies in the Valin River paleodelta, in: Proceedings of the 72nd Canadian Geotechnical Conference, St-John's, Newfoundland, Canada. p. 8.

Boumaiza, L., Rouleau, A., Cousineau, P.A., 2017. Determining hydrofacies in granular deposits of the Valin River paleodelta in the Saguenay region of Quebec, in: Proceedings of the 70th Canadian Geotechnical Conference and the 12th Joint CGS/IAH-CNC Groundwater Conference, Ottawa, Ontario, Canada. p. 8.

Boumaiza, L., Rouleau, A., Cousineau, P.A., 2015. Estimation de la conductivité hydraulique et de la porosité des lithofaciès identifiés dans les dépôts granulaires du paléodelta de la rivière Valin dans la région du Saguenay au Québec, in: Proceedings of the 68th

Canadian Geotechnical Conference, Quebec City, Quebec, Canada. p. 9.
Boumaiza, L., Walter, J., Chesnaux, R., Karthikeyan, B., Lakshmanan, E., Rouleau, A., Wachniew, P., Stumpp, C., 2021. An operational methodology for determining relevant DRASTIC factors and their relative weights in the assessment of aquifer vulnerability to contamination. Environmental Earth Sciences 80, 1–19. https://doi.org/doi.org/10.1007/s12665-021-09575-w
Box, G.E.P., Jenkins, G.M., Reinsel, G.C., 1994. Time Series Analysis: Forecasting and Control. Prentice Hall Inc., Englewood Cliffs, NJ, USA.
Brodersen, C., Pohl, S., Lindenlaub, M., Leibundgut, C., Wilpert, K.V., 2000. Influence of vegetation structure on isotope content of throughfall and soil water. Hydrological Processes 14, 1439–1448.
Cai, Z., Ofterdinger, U., 2016. Analysis of groundwater-level response to rainfall and estimation of annual recharge in fractured hard rock aquifers, NW Ireland. Journal of Hydrology 535, 71–84.
Carretero, S.C., Kruse, E.E., 2012. Relationship between precipitation and water-table fluctuation in a coastal dune aquifer: Northeastern coast of the Buenos Aires province, Argentina. Hydrogeology Journal 20, 1613–1621.
CERM-PACES, 2013. Résultats du programme d'acquisition de connaissances sur les eaux souterraines de la région Saguenay-Lac-Saint-Jean. Centre d'études sur les ressources minérales, Université du Québec à Chicoutimi.
Chesnaux, R., Elliott, A.P., 2011. Demonstrating evidence of hydraulic connections between granular aquifers and fractured rock aquifers, in: Proceedings of GeoHydro 2011, Joint Meeting of the Canadian Quaternary Association and the Canadian Chapter of the International Association of Hydrogeologists, August 28–31, 2011, Quebec City, Quebec, Canada. p. 8.
Chesnaux, R., Stumpp, C., 2018. Advantages and challenges of using soil water isotopes to assess groundwater recharge dominated by snowmelt at a field study located in Canada. Hydrological Sciences Journal 63, 679–695.
Chiaudani, A., Di Curzio, D., Palmucci, W., Pasculli, A., Polemio, M., Rusi, S., 2017. Statistical and fractal approaches on long time-series to surface-water/groundwater relationship assessment: A central Italy alluvial plain case study. Water (Switzerland) 9, 1–28.
Daigneault, R., Cousineau, P.A., Leduc, E., Beaudoin, G., Millette, S., Horth, N., Roy, D.W., Lamothe, M., Allard, G., Des, 2011. Rapport final sur les travaux de cartographie, Municipalisé, formations superficielles réalisés dans le territoire, Ministère, du S.-L.-S.-J.Q.C., Québec., des R. naturelles et de la F. du, 2011. Rapport final sur les travaux de cartographie des formations superficielles réalisés dans le territoire municipalisé du Saguenay-Lac-Saint-Jean. Ministère des Ressources naturelles et de la Faune du Québec, Canada.
Delbart, C., Valdes, D., Barbecot, F., Tognelli, A., Richon, P., Couchoux, L., 2014. Temporal variability of karst aquifer response time established by the sliding-windows cross-correlation method. Journal of Hydrology 511, 580–588.
Diggle, P.D., 1990. Times Series: A Biostatistical Introduction. Oxford Statistical Science Series. Oxford Science Publications.
Duffy, C.J., Gelhar, L.W., 1986. A Frequency Domain Analysis of Groundwater Quality Fluctuations: Interpretation of Field Data. Water Resources Research 22, 1115–1128.

Duvert, C., Jourde, H., Raiber, M., Cox, M.E., 2015. Correlation and spectral analyses to assess the response of a shallow aquifer to low and high frequency rainfall fluctuations. Journal of Hydrology 527, 894–907.

Government of Canada, 2019. Canada's national climate archive. http://www.climate.weatheroffice.ec.gc.ca/climate_normals/ [consulted in July 2019].

Hébert, C., Lacoste, P., 1998. Géologie de la région de Jonquière -Chicoutimi. Rapport géologique no. RG 96- 08, Ministère des Ressources Naturelles du Québec, Canada.

Hopmans, J.W., Nielsen, D.R., Bristow, K.L., 2002. How useful are small-scale soil hydraulic property measurements for large-scale vadose zone modeling?, in: Geophysical Monograph Series. pp. 247–258.

Horton, J.H., Hawkins, R.H., 1965. Flow path of rain from the soil surface to the water table. Soil Science 100, 377–383.

Hsien-tsung, L., Yih-chi, T., Chu-hui, C., Hwa-lung, Y., Shih-ching, W., Kai-yuan, K., 2010. Estimation of effective hydrogeological parameters in heterogeneous and anisotropic aquifers. Journal of Hydrology 389, 57–68.

Imagawa, C., Takeuchi, J., Kawachi, T., Chono, S., Ishida, K., 2013. Statistical analyses and modeling approaches to hydrodynamic characteristics in alluvial aquifer. Hydrological Processes 27, 4017–4027.

Jeong, J., Park, E., 2017. A shallow water table fluctuation model in response to precipitation with consideration of unsaturated gravitational flow. Water Resources Research 53, 3505–3512.

Konikow, L.F., 2011. The Secret to Successful Solute-Transport Modeling. Ground Water 49, 144–159.

Labrecque, G., Chesnaux, R., Boucher, M.A., 2020. Water-table fluctuation method for assessing aquifer recharge: application to Canadian aquifers and comparison with other methods. Hydrogeology Journal 28, 521–533.

Larocque, M., Mangin, A., Razack, M., Banton, O., 1998. Contribution of correlation and spectral analyses to the regional study of a large karst aquifer (Charente, France). Journal of Hydrology 205, 217–231.

Lasalle, P., Tremblay, G., 1978. Dépôts meubles du Saguenay Lac Saint-Jean. Rapport géologique n° 191, ministère des Richesses naturelles du Québec, Canada.

Laurin, A.F., Sharma, K.N.M., 1975. Mistassini, Peribonka, Saguenay Rivers Area: Grenville 1965–1967. Ministère des richesses naturelles, Direction générale des mines, Geological Exploration Service: Québec, QC, Canada.

Lee, L.J.E., Lawrence, D.S.L., Price, M., 2006. Analysis of water-level response to rainfall and implications for recharge pathways in the Chalk aquifer, SE England. Journal of Hydrology 330, 604–620.

Lozano-Parra, J., Schnabel, S., Ceballos-Barbancho, A., 2015. The role of vegetation covers on soil wetting processes at rainfall event scale in scattered tree woodland of Mediterranean climate. Journal of Hydrology 529, 951–961.

Meinken, W., Stober, I., 1997. Permeability distribution in the Quaternary of the Upper Rhine glacio-fluvial aquifer. Terra Nova 9, 113–116.

Owor, M., Taylor, R.G., Tindimugaya, C., Mwesigwa, D., 2009. Rainfall intensity and groundwater recharge: Empirical evidence from the Upper Nile Basin. Environmental Research Letters 4, 1–7.

Padilla, A., Pulido-Bosch, A., 1995. Study of hydrographs of karstic aquifers by means of

correlation and cross-spectral analysis. Journal of Hydrology 168, 73–89.
Pagé, P., 1999. Les grandes glaciations: l'histoire et la stratigraphie des glaciations continentales dans l'hémisphère Nord. Guérin Éditeur Ltée, Montréal (Québec), Canada.
Panagopoulos, G., Lambrakis, N., 2006. The contribution of time series analysis to the study of the hydrodynamic characteristics of the karst systems: Application on two typical karst aquifers of Greece (Trifilia, Almyros Crete). Journal of Hydrology 329, 368–376.
Parent, M., Occhietti, S., 1988. Late Wisconsinan Deglaciation and Champlain Sea Invasion in the St. Lawrence Valley, Québec. Géographie physique et Quaternaire 42, 215–246.
Pavlić, K., Parlov, J., 2019. Cross-correlation and cross-spectral analysis of the hydrographs in the northern part of the Dinaric karst of Croatia. Geosciences (Switzerland) 9, 1–15.
Potter, J., 1965. Water content of freshly fallen snow. Rep. CIR-4232, TEC-569, Meteorological Branch, Department of Transport, Toronto (Ontario) Canada.
Rathay, S.Y., Allen, D.M., Kirste, D., 2018. Response of a fractured bedrock aquifer to recharge from heavy rainfall events. Journal of Hydrology 561, 1048–1062.
Tam, V.T., De Smedt, F., Batelaan, O., Dassargues, A., 2004. Characterization of a cavern conduit system in Vietnam by time series correlation, cross-spectrum and wavelet analyses. Hydrological Sciences Journal 49, 879–900.
Tremblay, P., 2005. Étude hydrogéologique de l'aquifère de Saint-Honoré avec emphase sur son bilan hydrique [Hydrogeologic analysis of Saint-Honoré aquifer with emphasis on its water budge]. Master's Thesis, Université du Québec à Chicoutimi, Québec, Canada.
Turkeltaub, T., Kurtzman, D., Bel, G., Dahan, O., 2015. Examination of groundwater recharge with a calibrated/validated flow model of the deep vadose zone. Journal of Hydrology 522, 618–627.
Uchida, T., McDonnell, J.J., Asano, Y., 2006. Functional intercomparison of hillslopes and small catchments by examining water source, flowpath and mean residence time. Journal of Hydrology 327, 627–642.
Vereecken, H., Schnepf, A., Hopmans, J.W., Javaux, M., Or, D., Roose, T., Vanderborght, J., Young, M.H., Amelung, W., Aitkenhead, M., Allison, S.D., Assouline, S., Baveye, P., Berli, M., Brüggemann, N., Finke, P., Flury, M., Gaiser, T., Govers, G., Ghezzehei, T., Hallett, P., Hendricks Franssen, H.J., Heppell, J., Horn, R., Huisman, J.A., Jacques, D., Jonard, F., Kollet, S., Lafolie, F., Lamorski, K., Leitner, D., McBratney, A., Minasny, B., Montzka, C., Nowak, W., Pachepsky, Y., Padarian, J., Romano, N., Roth, K., Rothfuss, Y., Rowe, E.C., Schwen, A., Šimůnek, J., Tiktak, A., Van Dam, J., van der Zee, S.E.A.T.M., Vogel, H.J., Vrugt, J.A., Wöhling, T., Young, I.M., 2016. Modeling Soil Processes: Review, Key Challenges, and New Perspectives. Vadose Zone Journal 15, 1–57.
Vero, S.E., Healy, M.G., Henry, T., Creamer, R.E., Ibrahim, T.G., Richards, K.G., Mellander, P.E., McDonald, N.T., Fenton, O., 2017. A framework for determining unsaturated zone water quality time lags at catchment scale. Agriculture, Ecosystems and Environment 263, 234–242.
Vienken, T., Dietrich, P., 2011. Field evaluation of methods for determining hydraulic conductivity from grain size data. Journal of Hydrology 400, 58–71.
Wakode, H.B., Baier, K., Jha, R., Azzam, R., 2018. Impact of urbanization on groundwater recharge and urban water balance for the city of Hyderabad, India. International Soil and Water Conservation Research 6, 51–62.

Walter, J., Chesnaux, R., Cloutier, V., Gaboury, D., 2017. The influence of water/rock − water/clay interactions and mixing in the salinization processes of groundwater. Journal of Hydrology: Regional Studies 13, 168–188.